J|A|C|S
ARTICLES
Published on Web 09/09/2006

Reversible pH-Driven Conformational Switching of Tethered Superoxide Dismutase with Gold Nanoparticle Enhanced Surface Plasmon Resonance Spectroscopy

Taewook Kang,[‡] Surin Hong,[‡] Inhee Choi,[‡] Jung Jun Sung,[†] Younjung Kim,[‡] Ji-Sook Hahn,[‡] and Jongheop Yi*[,‡]

Contribution from the College of Medicine and School of Chemical and Biological Engineering, Institute of Chemical Processes, Seoul National University, San 56-1, Shillim, Kwanak, Seoul 151-742, Korea

Received May 8, 2006; E-mail: jyi@snu.ac.kr

Abstract: A new class of surface-immobilized protein nanomachines can be reversibly actuated by cycling the solution pH between 2.5 and 12.3, which induces a conformational change, thereby modulating the thickness of superoxide dismutase (SOD1) tethered to the Au thin film. By placing Au nanoparticles (AuNP) atop the immobilized SOD1 by means of a gold−thiol assembly, the nanoscale motion of SOD1 at the interface produces mechanical work to lift and then lower the AuNP from the Au substrate by a distance of ca. 3 nm and transduces this motion into an easily measurable reflectivity change in the surface plasmon resonance (SPR) spectrum. As-made supported conjugate consisting of SOD1 and AuNP is quite robust and stable, and its operation in response to pH variations, which mirrors the conformational changes of responsive SOD1 at the interface, is found to be highly reversible and reproducible. This is the first demonstration of the development of novel solid-state sensors and/or switching devices based on substrate-bound protein conformational changes and AuNP enhanced SPR spectroscopy.

Introduction

Knowledge of how biomolecules fold, from a biological point of view, contributes to our understanding of the causes of certain types of diseases and, thus, to develop corresponding therapeutic treatments.[1] On the other hand, from the application point of view, conformational changes of biomolecules, which result from the intrinsic flexibility of their structures, have the potential to be exploited to develop new types of bio-nanomechanical devices. Conformational switching from the original native structure of biomolecules, such as proteins and nucleic acids, upon exposure to external stimuli has been recently demonstrated to be of major importance in the design of molecular machines and stimuli-responsive materials.[2−4]

For example, DNA-based artificial nanomotors and nanomachines have been shown to be capable of producing reversible, well-defined nanometer-scale motions, which may facilitate their further applications as sensors or switch junctions in nanoelectronic devices.[5−7] Despite the wide variety of structural motifs used as DNA nanomechanical devices, the various modules share some common underlying principles in terms of conformational transitions, such as the formation of duplexes and other secondary structures through hybridization (via base pairing or strand replacement), which can be induced by the external stimuli. However, most of these DNA motors and machines are fueled by either competitive hybridization or proton and can be susceptible to system poisoning due to the accumulation of waste duplex DNA and the presence of complementary strands in solution.

In this regard, the conformational switching of proteins in a reversible, repeatable, and stable manner from the conformational transition, from their native state to an altered state (e.g., from structurally compact to comparatively loose), can serve as an alternative source to produce mechanical work at the molecular level. With appropriate choice of the principle of signal transduction, this possibility gives rise to a potentially new class of molecular machines and sensors, thus adding to those that are based on DNA.

Several criteria need to be met in order to exploit such conformational transitions of proteins in a practical way. First, it is necessary that they be organized at the interfaces, deposited

[†] College of Medicine, Seoul National University.
[‡] School of Chemical and Biological Engineering, Seoul National University.

(1) (a) Lindberg, M. J.; Normark, J.; Holmgren, A.; Oliveberg, M. *Proc. Natl. Acad. Sci. U.S.A.* **2004**, *101*, 15893. (b) Julien, J. P. *Cell* **2001**, *104*, 581. (c) Baskakov, I. V.; Legname, G.; Prusiner, S. B.; Cohen, F. E. *J. Biol. Chem.* **2001**, *276*, 19687. (d) Cole, N. B.; Murphy, D. D.; Grider, T.; Rueter, S.; Brasaemle, D.; Nussbaum, R. L. *J. Biol. Chem.* **2002**, *277*, 6344.
(2) (a) Seeman, N. C. *Nature* **2003**, *421*, 427. (b) Simmel, F. C.; Dittmer, W. U. *Small* **2005**, *1*, 284.
(3) Feldkamp, U.; Niemeyer, C. M. *Angew. Chem., Int. Ed.* **2006**, *45*, 1856.
(4) Chah, S.; Hammond, M. R.; Zare, R. N. *Chem. Biol.* **2005**, *12*, 323.
(5) (a) Mao, C. D.; Sun, W. Q.; Shen, Z. Y.; Seeman, N. C. *Nature* **1999**, *397*, 144. (b) Yan, H.; Zhang, X.; Shen, Z.; Seeman, N. C. *Nature* **2002**, *415*, 62. (c) Li, J. J.; Tan, W. H. *Nano Lett.* **2002**, *2*, 315. (d) Alberti, P.; Mergny, J. L. *Proc. Natl. Acad. Sci. U.S.A.* **2003**, *100*, 1569.
(6) (a) Bath, J.; Green, S. J.; Turberfield, A. J. *Angew. Chem., Int. Ed.* **2005**, *44*, 4358. (b) Tian, Y.; Mao, C. D. *J. Am. Chem. Soc.* **2004**, *126*, 11410. (c) Chen, Y.; Wang, M. S.; Mao, C. D. *Angew. Chem., Int. Ed.* **2004**, *43*, 3554. (d) Shin, J.-S.; Pierce, N. A. *J. Am. Chem. Soc.* **2004**, *126*, 10834.
(7) (a) Liu, D.; Bruckbauer, A.; Abell, C.; Balasubramanian, S.; Kang, D.-J.; Klenerman, D.; Zhou, D. *J. Am. Chem. Soc.* **2006**, *128*, 2067. (b) Liedl, T.; Simmel, F. C. *Nano Lett.* **2005**, *5*, 1894.

 10.1021/ja0632198 CCC: $33.50

on surfaces, or immobilized on membranes or porous materials. In these cases, their conformations on the surface should be regarded as projections of their conformations in solution. Second, the physicochemical stability of tethered proteins should be sufficiently high to permit their function to be retained upon in vitro immobilization, and their conformational switching must be preserved under operating conditions employed (e.g., temperature, pH, multiple runs, etc.). However, the behavior of biomolecules at interfaces is often significantly different from their behavior in bulk or in solution.[8] At interfaces or surfaces, biomolecules are unable to assume the full range of conformations available to an unconstrained molecule and can lead to the formation of different, nonequilibrium structures, and in even some cases, protein−surface interactions may cause proteins to unfold.[9,10]

On the basis of these considerations, we selected copper−zinc superoxide dismutase (CuZnSOD, SOD1) as a test molecule, due to its physicochemical stability.[11] Furthermore, SOD1 at Au electrodes has been well studied using its unique electrocatalytic activity[12] (i.e., catalyzing the dismutation of the superoxide anion ($O_2^{\bullet-}$) to O_2 and H_2O) as a potential approach to the in vivo detection of $O_2^{\bullet-}$. In other words, this demonstrates that SOD1 retains its activity, which is closely related with the stability when it is immobilized in vitro. SOD1, a 32 kDa homodimer, is ubiquitous in the cytosol, nucleus, peroxisomers, and mitochondrial intermembrane space of human cells. The dimer is an elongated ellipsoid about 33 Å wide, 67 Å long, and 36 Å deep.[12a,13]

Here, we took advantage of the intrinsic conformational changes of immobilized SOD1, induced by changing the solution pH. To convert its conformational transition into a measurable output, Au nanoparticles (AuNP) were placed atop the SOD1 tethered to a Au film, and surface plasmon resonance (SPR)[14−18] was applied as signal transduction principle. In this case, we further utilized the dynamic distance between the AuNP and the Au surface modulated by the conformational changes of SOD1 upon pH alteration. Because the changes in the dynamic distance between them drastically alter the SPR response (e.g., minimum reflectivity and/or SPR angle shift),[19−21] the conformational transition is therefore accompanied by a significant variation in the SPR response.

Materials and Methods

Materials. 11-Mercaptoundecanoic acid (MUA, Sigma-Aldrich), hexanedithiol (HDT, Aldrich), *N*-(3-dimethylaminopropyl)-*N*′-ethylcarbodiimide hydrochloride (EDC, Aldrich), and *N*-hydroxysuccinimide (NHS, Sigma-Aldrich) were used as received. Urea (Sigma) was dissolved in 25 mM potassium phosphate buffer (PBS, pH 7.4) to prepare urea solutions of different concentrations up to 2 M. H_2O was purified to above 18 MΩ using a Milli-Q water system (Millipore).

SPR Instrumentation. Figure S1 shows a schematic representation of the reaction cell used in the SPR instrumentation. A flow cell is mounted on the sensor/prism assembly so that solutions to be subjected to inducing the conformational changes of tethered protein can be introduced easily and flow across the Au surface, thus permitting switching between different solutions to occur rapidly. We utilized a six-phase, denoted as a (012345) SPR system in the Kretschmann configuration using attenuated total reflection (ATR). The different phases are labeled as follows: 0, BaK prism ($n = 1.566706$); 1, a layer of Au thin film (50 nm); 2, a carboxylic acid-terminated self-assembled monolayer (SAM) of MUA; 3, a layer of supported SOD1; 4, adsorbed AuNP; 5, an ambient dielectric medium of buffer (25 mM PBS buffer). Time-resolved SPR angle shifts were measured using the fixed angle method. Reflectance data at a fixed incident angle were acquired in real time on a computer. For further calculation, the angle of incidence (θ in Figure S1) was calculated from Snell's law ($n_i \sin \theta_i = n_j \sin \theta_j$).

SOD1 Purification. Human SOD genes encoding the wild type were cloned into the pET23b(+) (Novagen) vector, and the proteins were expressed in *E. coli* BL21(DE3)pLysS.[22] Cultures were induced by treatment with 0.5 mM isoprophyl β-D-thiogalactopyranoside for 3−6 h at 30 °C, and the cells were lysed by sonication in a buffer containing 150 mM NaCl, 50 mM Tris-HCl (pH 8.0), 0.1 mM EDTA, 1 mM dithiothreitol (DTT), and 1 mM phenylmethylsulfonyl fluoride (PMSF). Solid $(NH_4)_2SO_4$ was added to the cell extracts to ∼50% saturation (0.313 g/mL), and after centrifugation, the supernatant proteins were loaded on a phenyl-sepharose 6 Fast Flow high subhydrophobic column (Amersham Biosciences). Proteins were eluted with a linear gradient of ammonium sulfate (0.75−0 M) in 50 mM sodium phosphate (pH 7.0), 150 mM NaCl, 0.1 mM EDTA, and 0.25 mM DTT. Wild type SOD1 was released with a high specificity from the column between 1.3 and 0.8 M ammonium sulfate.

Human SOD1 Immobilization on the Au Thin Film. The immobilization procedures utilized carboxylate-modified (MUA-coated) surfaces to covalently attach proteins to the Au thin film via traditional carbodiimide coupling to protein-free amine moieties.[9a,23,24] The overall experimental procedures are summarized in Figure S2. In a typical experiment, a self-assembled monolayer (SAM) of MUA on the Au thin film was formed by treatment with a 1 mM ethanolic solution of MUA for 18 h. The formation of an MUA monolayer was investigated by SPR measurements and auger electron spectroscopy (AES). For the immobilization of SOD1 on the MUA-treated Au thin film by covalent bonding, the MUA-treated surface was first activated by a 7 min exposure to a 1:1 mixture of 0.4 M EDC and a 0.1 M aqueous solution of NHS. SOD1 (0.1 mM), in the same buffer solution, was then used for the immobilization (4 h). The immobilization of SOD1 was investigated by angle- (Figure S3) and time-resolved SPR measurements. At saturation, the surface was rinsed with copious amounts of water and buffer solution.

Au Nanoparticle Immobilization of SOD1/Au. Colloidal Au nanoparticles (20 nm diameters) were prepared by the reduction of

(8) Zhu, H.; Snyder, M. *Curr. Opin. Chem. Biol.* **2003**, *7*, 55.
(9) (a) Kang, T.; Hong, S.; Kim, H. J.; Moon, J.; Oh, S.; Paik, S. R.; Yi, J. *Langmuir* **2006**, *22*, 13. (b) Sadana, A. *Chem. Rev.* **1992**, *92*, 1799.
(10) Chah, S.; Kumar, C. V.; Hammond, M. R.; Zare, R. N. *Anal. Chem.* **2004**, *76*, 2112.
(11) Valentine, J. S.; Doucette, P. A.; Potter, S. Z. *Annu. Rev. Biochem.* **2005**, *74*, 563.
(12) (a) Tian, Y.; Mao, L.; Okajima, T.; Ohsaka, T. *Anal. Chem.* **2004**, *76*, 4162. (b) Tian, Y.; Mao, L.; Okajima, T.; Ohsaka, T. *Anal. Chem.* **2002**, *74*, 2428.
(13) Tainer, J. A.; Getzoff, E. D.; Beem, K. M.; Richardson, D. C. *J. Mol. Biol.* **1982**, *160*, 181.
(14) (a) Knoll, W. *Annu. Rev. Phys. Chem.* **1998**, *49*, 569. (b) Wischerhoff, E.; Zacher, T.; Laschewsky, A.; Rekai, E. D. *Angew. Chem., Int. Ed.* **2000**, *39*, 4602.
(15) Barnes, W. L.; Dereux, A.; Ebbesen, T. W. *Nature* **2003**, *424*, 824.
(16) (a) Kang, T.; Hong, S.; Moon, J.; Oh, S.; Yi, J. *Chem. Commun.* **2005**, 3721. (b) Kang, T.; Moon, J.; Oh, S.; Hong, S.; Chah, S.; Yi, J. *Chem. Commun.* **2005**, 2360.
(17) Jung, L. S.; Campbell, C. T.; Chinowsky, T. M.; Mar, M. N.; Yee, S. S. *Langmuir* **1998**, *14*, 5636.
(18) (a) Roy, D.; Fendler, J. H. *Adv. Mater.* **2004**, *16*, 479. (b) Chah, S.; Fendler, J. H.; Yi, J. *Chem. Commun.* **2002**, 2094.
(19) (a) Lyon, L. A.; Musick, M. D.; Natan, M. J. *Anal. Chem.* **1998**, *70*, 5177. (b) He, L.; Musick, M. D.; Nicewarner, S. R.; Salinas, F. G.; Benkovic, S. J.; Natan, M. J.; Keating, C. D. *J. Am. Chem. Soc.* **2000**, *122*, 9071. (c) Lyon, L. A.; Holliway, W. D.; Natan, M. J. *Rev. Sci. Instrum.* **1999**, *70*, 2076.
(20) Hutter, E.; Fendler, J. H.; Roy, D. *J. Phys. Chem. B* **2001**, *105*, 11159.
(21) He, L.; Smith, E. A.; Natan, M. J.; Keating, C. D. *J. Phys. Chem. B* **2004**, *108*, 10973.
(22) Boissinot, M.; Karnas, S.; Lepock, J. R.; Cabelli, D. E.; Tainer, J. A.; Getzoff, E. D.; Hallewell, R. A. *EMBO J.* **1997**, *16*, 2171.
(23) Su, X.; Wu, Y.-J.; Robelek, R.; Knoll, W. *Langmuir* **2005**, *21*, 348.
(24) Lahiri, J.; Isaacs, L.; Tien, J.; Whitesides, G. M. *Anal. Chem.* **1999**, *71*, 777.

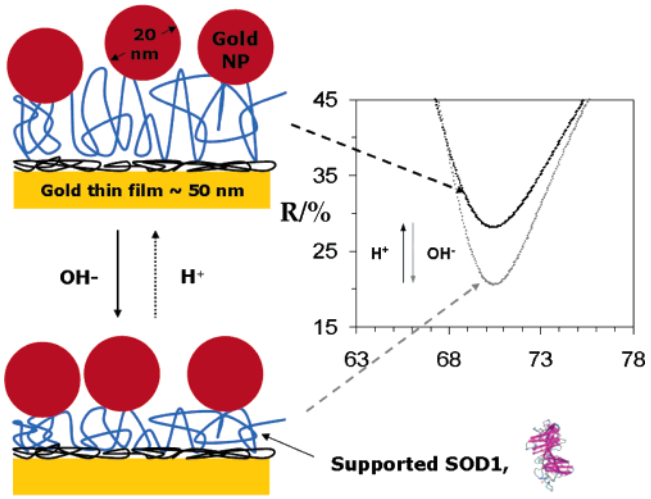

Figure 1. Left: Schematics of the reversible pH-driven conformational switching of tethered superoxide dismutase (SOD1) to Au nanoparticles (AuNP) (dimensions not to scale). Right: Corresponding SPR spectra of the immobilized SOD1 with AuNP on a Au thin film.

$HAuCl_4 \cdot 3H_2O$ with citrate as previously described.[25] Optical spectra with $\lambda_{max} = 530$ nm and a full peak width at half-maximum of ~84 nm were recorded using a Hewlett-Packard 8453 spectrophotometer (Figure S4). Aqueous suspensions of the particles render the color of the suspension red. The SOD1 monomer contains four cysteine residues, at positions 6, 57, 111, and 146 of which residues 57 and 146 form a disulfide linkage in the native state. Because SOD1 contains the free cysteine residues, this feature can be utilized to self-assemble Au nanoparticles (AuNP) on the SOD1 (via a gold−thiol assembly technique). The SOD1-covered Au substrates were exposed to an aqueous dispersion of AuNP. The deposition of the AuNP on SOD1 was monitored by SPR and AFM.

Liquid-AFM Characterization. The use of AFM to examine in biological or chemical samples in liquid media can be very useful because (i) the oscillating energy activated between the tip and sample in the tapping mode are reduced, and (ii) structural changes in macromolecules can be observed in their native environment. To scan a sample in the liquid phase, commercially available liquid cells have been developed by several researchers. In this work, an open liquid-cell system, in conjunction with a commercial AFM instrument (XE-100, PSIA, Korea), was used.[26] To minimize intrinsic distortions of the apparatus, an independent *z*-scanner was used, which also eliminates the *x*−*z* cross-coupling problem that is inherent in conventional AFM.

Results and Discussion

Figure 1 illustrates the scheme for the reversible actuation of tethered SOD1 modified with Au nanoparticles (AuNP) on a Au thin film, hereafter referred to as AuNP/SOD1/Au. Our design for AuNP/SOD1 conjugate formation is based on the immobilization (via amide bond formation) of SOD1 on a thin Au (~50 nm)-coated glass and subsequent attachment of AuNP (via a gold−thiol self-assembly) onto the SOD1/Au film. To follow the formation of these assemblies on the surface of the Au thin film, each reaction was monitored by angle- and time-resolved SPR measurements. Figure 2 shows the time-resolved SPR curve for the attachment of SOD1 on the Au thin film

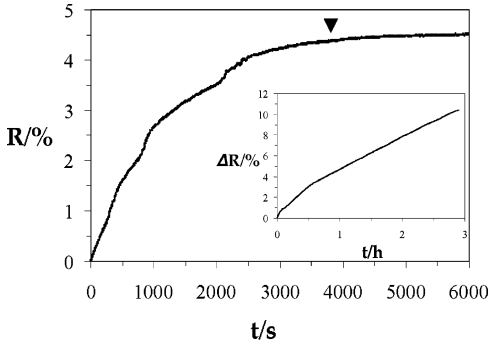

Figure 2. Time-resolved SPR curve (differential reflectance time courses) corresponding to the immobilization of SOD1 on a Au film. Inset: Change in reflectance at the fixed angle of a SOD1-derivatized Au film measured during exposure to a 20 nm Au colloid.

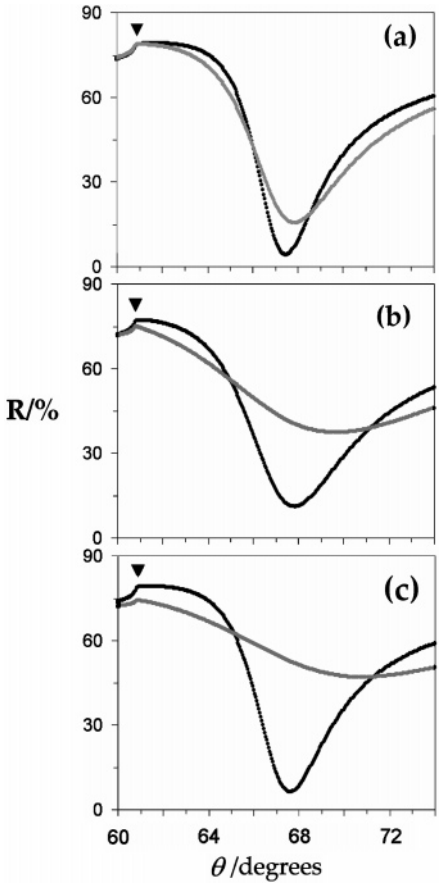

Figure 3. SPR curves (reflectance versus angle) for a Au thin film with SOD1 and 20 nm diameter colloidal Au for varying exposure times: (a) 3 h, (b) 5 h, and (c) 12 h. All SPR spectra were obtained in PBS buffer.

using an ambient dielectric of 25 mM PBS buffer. SOD1 began to be adsorbed immediately after the Au surface came into contact with the SOD1 solution (0.1 mM), reaching equilibrium in about 1 h, which eventually moved the angle-resolved SPR spectrum by 0.5° to the right (Figure S3). This change in resonance condition corresponds to ~82 ng of attached protein/cm^2.[27] By contrast, when the time course of the reflectance change was monitored at a fixed angle for the immobilization of AuNP to the SOD1/Au surface, the rate of adsorption was found to be fairly constant, while a ~10% reflectance change was easily observed in the first 2.5 h of the colloid AuNP adsorption (inset to Figure 2).

(25) (a) Handley, D. A. Methods for Synthesis of Colloidal Gold. In *Colloidal Gold: Principles, Methods and Applications*; Hayat, M. A., Ed.; Academic Press: San Diego, 1989. (b) Chah, S.; Fendler, J. H.; Yi, J. *J. Colloid Interface Sci.* **2002**, *250*, 142.
(26) (a) Kim, Y.; Choi, I.; Kang, S. K.; Lee, J.; Yi, J. *Rev. Sci. Instrum.* **2006**, *77*, 36114. (b) Kim, Y.; Kang, S. K.; Choi, I.; Lee, J.; Yi, J. *Appl. Phys. Lett.* **2006**, *88*, 173121.

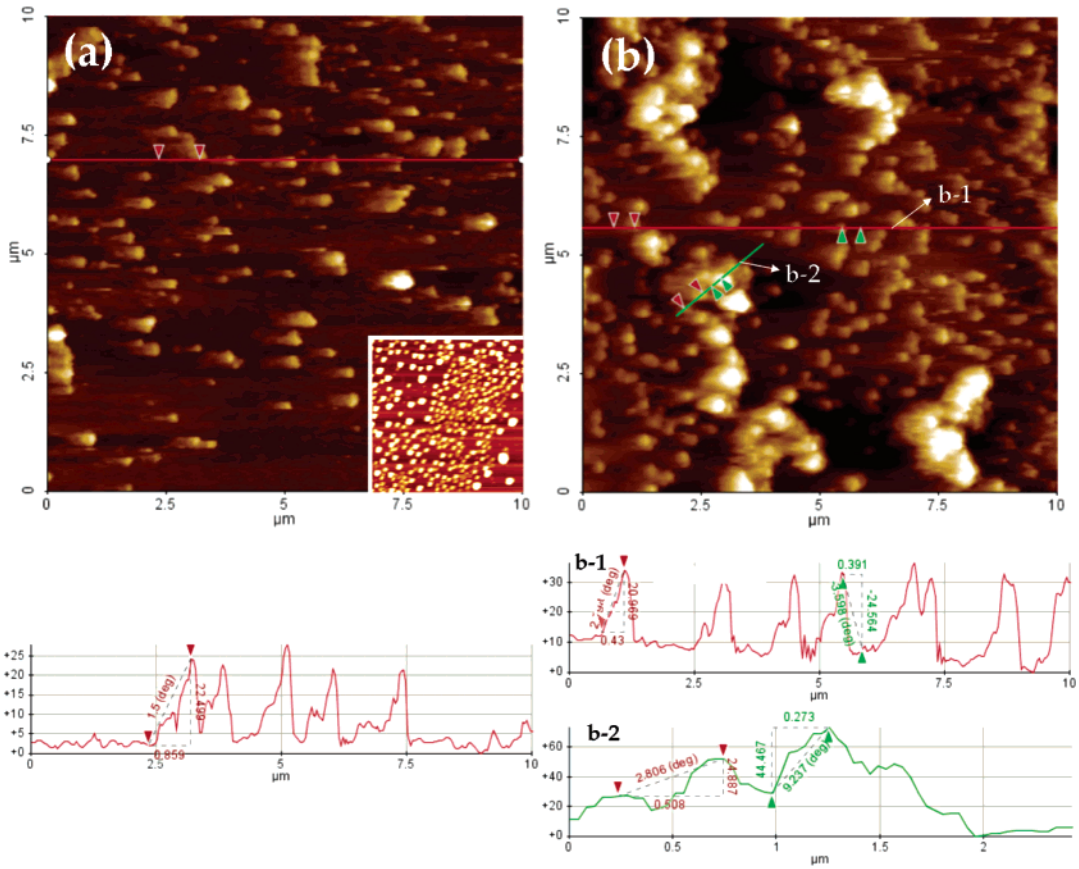

Figure 4. Top: Topographical AFM images (image size = 10 × 10 m^2) of the surfaces of SOD1/Au after exposure to the AuNP solution for (a) 3 h and (b) 12 h. The intermediate exposure time (5 h) is omitted for the sake of clarity. Inset to (a): Representative AFM topographic image (10 × 10 μm^2 scan area) taken in air from a concomitantly prepared silicon wafer after the immobilization of SOD1. For a comparison, a silicon wafer was used as a substrate for the case of the immobilization of SOD1. Because the surface [a root-mean-square (rms) roughness < 0.1 nm] of a silicon wafer is flatter than that (rms roughness ~ 0.6 nm) of a Au film, in this case, the immobilized SOD1 was easily discernible. Bottom: Corresponding typical linear scans along the scan direction indicated in (a) and (b).

The magnitude of this effect is further illustrated in the exposure time dependence of the SPR contour plots (Figure 3), which clearly showed a significant perturbation in the SPR response in terms of SPR angle shift and reflectance loss with increasing immersion time. The SPR curve of the SOD1-derivatized Au film is characterized by a sharp plasmon minimum at an angle of 67.5−67.8° for each Au substrate. Exposure of the SOD1/Au film to a solution of 20 nm diameter AuNP for 3 h resulted in an increase in the minimum reflectance, broadening of the curve, and a 0.4° shift in the plasmon angle (Figure 3a). Figure 3b and c shows that, with longer exposure times, the magnitude of these changes is increased; a 12 h exposure results in a shift in the plasmon angle to 70.8°, while the minimum reflectance increased by nearly 40% over that of the SOD1/Au film. It seems likely that an increase in the areal density of the tethered AuNP with increasing immersion time is responsible for the observed variation in the SPR responses.

To better understand this observation and to ensure appropriate visual correlation with the SPR data for the immobilization of AuNP, AFM was used to monitor changes in the surface morphologies of SOD1/Au before and after exposure to the AuNP solution, as shown in Figure 4. When the AFM image of an area covered with AuNP/SOD1 conjugate is compared with that of a bare Au surface, the two distinctive features of AuNP/SOD1 are (1) the appearance of numerous small, isolated islands, and (2) the size of these islands, which closely mimics the dimensions of the SOD1/Au (inset to Figure 4a) and remains unchanged irrespective of the immersion time, whereas the areal density of the tethered AuNP increases. For the case in which the tip curvature is comparable to the interparticle spacing between the tethered AuNP, an individual AuNP is not discernible because the lateral dimensions of the object of interest measured in the AFM topograph include the AFM tip convolution, which is likely to enlarge the lateral size of the object.[29] Therefore, to ensure an accurate size determination (also confirm the immobilization of the AuNP), only height measurements were used in the data analyses. As expected, section analyses shown in Figure 4a-1 and 4b-2 indicate that, taking into account the size of SOD1, the relative height of the

(27) In a calculation, the morphology of SOD1 is assumed to be equivalent to a spherical inclusion with a radius of 21.5 Å, although dimeric SOD1 is a somewhat elongated ellipsoid. To correlate the SPR spectra to the amount of the immobilized SOD1 on the Au surface, the Maxwell-Garnett theory[28] [for a two-constituent composite (in this case, pure SOD1 and buffer), the effective dielectric constant, $(\epsilon_{eff} - \epsilon_h)/(\epsilon_{eff} + 2\epsilon_h) = f(\epsilon_i - \epsilon_h)/(\epsilon_i + 2\epsilon_h)$, where ϵ_i and ϵ_h are the dielectric constants of constituents i and h, respectively, f represents the volume fill fraction of the inclusion, i] is employed here. Once the effective dielectric constants of SOD1 solution and the immobilized SOD1 layer for each case were determined through a simulated fit based on applying the Fresnel equation to the measured SPR spectra, using the Maxwell-Garnett equation, the amount of SOD1 immobilized on the Au film can be estimated.

(28) (a) Maxwell-Garnett, J. C. *Philos. Trans. R. Soc. London* **1904**, *203*, 385; **1906**, *205*, 237. (b) Gehr, R. J.; Boyd, R. W. *Chem. Mater.* **1996**, *8*, 1807.
(29) (a) Casero, E.; Darder, M.; Díaz, D. J.; Pariente, F.; Martín-Gago, J. A.; Abruña, H.; Lorenzo, E. *Langmuir* **2003**, *19*, 6230. (b) Erts, D.; Polyakov, B.; Olin, H.; Tuite, E. *J. Phys. Chem. B* **2003**, *107*, 3591.

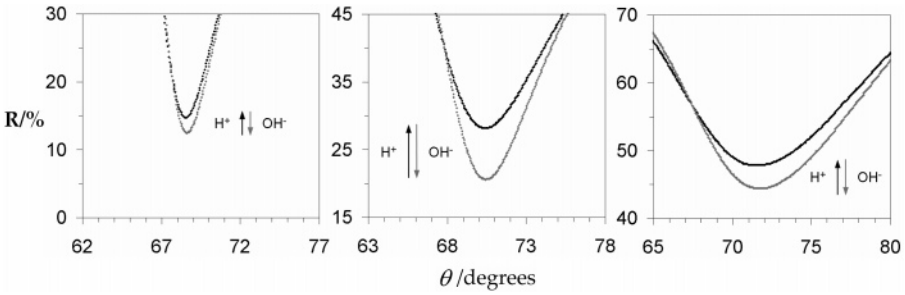

Figure 5. Representative in situ SPR spectra at pH 2.5 and 12.3 corresponding to a Au thin film with SOD1 and AuNP presented in Figure 3. All SPR spectra were directly taken in the incubation solution (not air).

feature to the baseline in a range of 22−24 nm is consistent with the known size of AuNP and also suggest that, within an individual island, the interparticle spacing of the tethered AuNP is smaller than ~10 nm. Note that a longer exposure time results in the appearance of a multilayered AuNP as well as the more populated monolayer regime for the AuNP (Figure 4b) rather than a monotonous expansion of the AuNP monolayer regime. The cursor plot displayed in Figure 4b-2 exhibits that the heights of the two selected islands are the multiples (2-fold and 3-fold) of the known size of the AuNP. Together, we found that most the AuNP multilayers tended to form after the AuNP occupied the entire region of the pre-immobilized SOD1, and AuNP without the intervening SOD1 layer was not immobilized on the bare Au surface (data not shown). This in turn suggests that the AuNP is site-selectively deposited on the regime of the immobilized SOD1.

To investigate the possibility of the reversible operation of as-made AuNP/SOD1/Au in response to the pH variation, AuNP/SOD1/Au was immersed in an aqueous solution at pH 12.3 and 2.5, and changes were examined by SPR measurements. In Figure 5, SPR spectra of the Au thin film with SOD1 and AuNP show a characteristic response to the pH alteration between pH 2.5 and 12.3, whereas no changes in the SPR response from the Au film with SOD1 in the absence of the AuNP were observed when the pH was switched between 2.5 and 12.3 for the control. Concerning AuNP/SOD1/Au, replacing the pH 12.3 solution with a pH 2.5 solution produced upward shifts in the percent reflectivity (*%R*) without any noticeable SPR angle shifts, and vice versa. Thus, the process appears to be highly reversible: the reflectivity at SPR angle increases when the solution pH is changed to 2.5 but is fully recovered when the pH is changed back to 12.3. The switching process between the native and the acid-denatured conformations is complete in less than 5 min. The magnitude of the *%R* exhibits nonlinearity with the exposure time of the AuNP solution; that is, the operational amplitude [$\Delta\%R = ((R_{min}/R_o)_{pH2.5} - (R_{min}/R_o)_{pH12}) \times 100$] initially increases in proportion to the immersion time in the AuNP solution and, after reaching a limiting value (~12%), with a further increase in immersion time up to 12 h, a decrease in $\Delta(R_{min}/R_o)$ is apparent. Noteworthy, the maximum change in $\Delta\%R$ is observed at the intermediate time of 5 h. The origin of the maximum response of $\Delta\%R$ appearing at an intermediate immersion time of the AuNP is not yet clear, but it is presumably associated with the formation of the AuNP multilayer on SOD1, which may hinder conformational changes of SOD1 due to an increase in the mass load on SOD1. It should be noted that, since conventional SPR imaging readily differentiates $\Delta\%R$ of ~1% (usually <5%) by the image contrast (dark to bright),[30,31] the change in $\Delta\%R$ of 12% upon the pH alteration in our system can be easily visualized by the naked eye and further utilized as a optical pH sensor as well as for the optical detection of the conformational change of the tethered protein. In our case, the transition from the native state (high pH) to the acid-denatured state (low pH) is signaled by the switching on of the reflectivity (bright). On the other hand, the reverse transition, induced by adjusting the pH value back to 12.3, is signaled by switching off (dark).

Measurements of the SPR spectra at different pH values produced titration curves (reflectivity at the resonance angle versus solution pH) as shown in Figures 6 and 8a. The immersion time dependences of the SPR response are displayed in Figures 6a, 6b, and 8a, which correspond to 12, 3, and 5 h, respectively. Apparent two-state transitions were observed for exposure times of 5 and 12 h. Note that the pH-induced shift in the reflectivity in the SPR spectra does not suffer from hysteresis. As expected, the variation in reflectance at the SPR resonance angle seen in Figures 6a, 6b, and 8a are not observed when the pH-dependent SPR measurements are repeated using the SOD1/Au substrate without AuNP (Figure 6c), with all other experimental conditions unchanged. This indicates that the observed reflectivity changes indeed are due to the AuNP/SOD1 conjugate.

To further verify that the operation is only specific for a conformational change in the tethered SOD1, a Au thin film modified with 1,6-hexanedithiol (HDT) and AuNP (AuNP/HDT/Au) was used as a control because HDT does not undergo conformational changes, such as denaturation and renaturation, with pH change. No variation in the SPR response (reflectivity and SPR angle shift) was found when the solution pH was changed (not shown here). This verifies that, although the introduction of AuNP on the immobilized SOD1 is responsible for the creation of optical pH responsiveness, the pH-induced conformational changes of the tethered SOD1 are essential for the actuation of the AuNP/SOD1 conjugate.

The following scenario may explain the insensitivity of the SPR response for the case without AuNP. On the basis of the assumption that SOD1 is a nonabsorbing dielectric,[32] the SPR response (thus, the SPR resonance angle (θ_{SPR})) increases as a function of both the thickness ($d_{SOD1layer}$) and the dielectric constant ($\epsilon_{SOD1layer}$) of the adlayer of SOD1 on the Au.[33,34] From

(30) Brockman, J. M.; Nelson, B. P.; Corn, R. M. *Annu. Rev. Phys. Chem.* **2000**, *51*, 41.
(31) Goodrich, T. T.; Lee, H. J.; Corn, R. M. *J. Am. Chem. Soc.* **2004**, *126*, 4086.
(32) Under this assumption, SOD1 does not make any contribution to the reflection loss of the SPR curve because of the zero absorption coefficient in its refractive index.

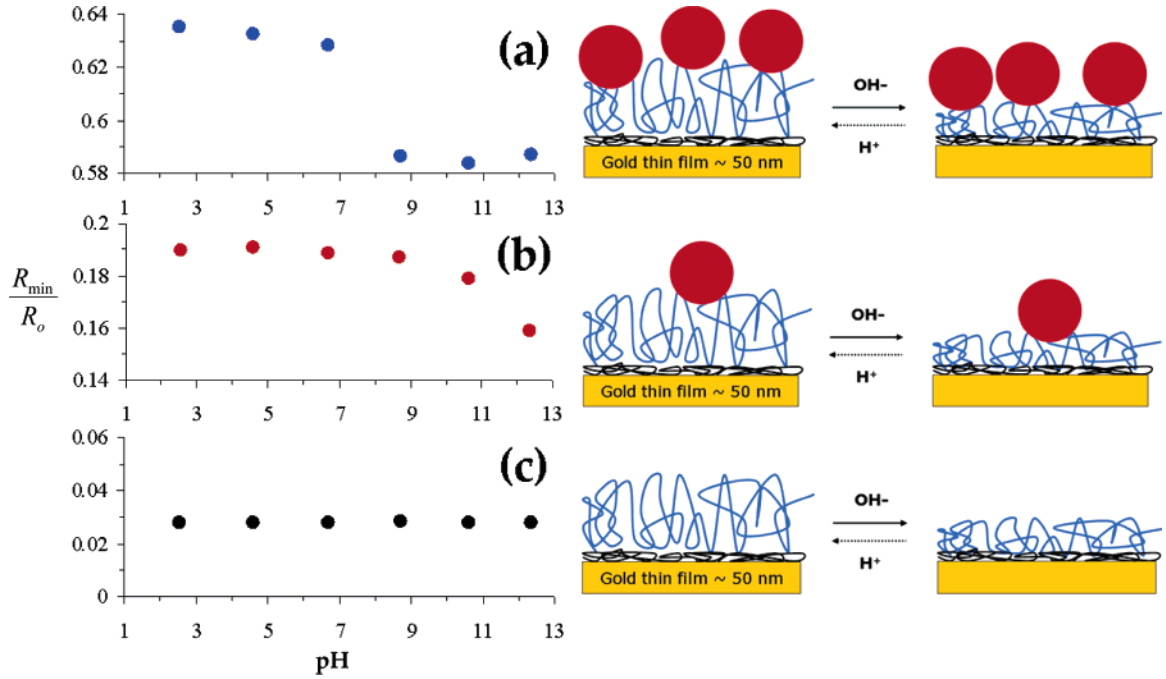

Figure 6. Left: Titration curves (shift of the reflectivity minimum of the SPR spectra) as a function of pH, which corresponds to AuNP/SOD1/Au obtained from the exposure times of (a) 12 h and (b) 3 h. (c) Corresponds to Au thin film with SOD1 in the absence of AuNP. Right: The cartoons represent the corresponding surface status.

the SPR observations, we can infer that, for the case of the pH-triggered conformational changes of SOD1, a situation can exist where the effects can vary in magnitude resulting in opposing tendencies. In other words, with an increase in $d_{SOD1layer}$ (e.g., if the pH alteration induces stretching of the polypeptide chain), the effective dielectric constant, $\epsilon_{SOD1layer}$, decreases simultaneously (this is the case where the dielectric constant of the solvent molecule is lower than that of SOD1), and this effect offsets the net change in SPR response due to the increase in thickness, and eventually, it would not be possible to detect the pH-triggered conformational changes of the tethered SOD1 by the transduction principle of SPR. An analogous situation of dielectric constant and thickness reversal has been reported, for example, for a surface-attached polymer (polymer brush).[34]

If the stimulus-induced conformational changes actuate the AuNP/SOD1 conjugate, then, it would be expected that a similar enhancement in SPR response to the stimulus-triggered conformational changes would be observed for the case in which another denaturant replaces the pH. To verify this, AuNP/SOD1/Au was incubated with a urea solution. Figure 7 provides a plot of reflectivity at the resonance angle as a function of urea concentration. Upon denaturation by the urea, no significant change in reflectance was observed as the concentration of the urea was increased from 0 to 2 M for the SOD1/Au film without AuNP, whereas a dramatically enhanced shift (20-fold) in reflectivity is observed if AuNP is adsorbed to the tethered SOD1.

As stated above, the operational amplitude ($\Delta\%R$) among the three AuNP/SOD1/Au samples was found to be optimized in the 5 h exposure to the AuNP solution. Accordingly, 5 h of the AuNP/SOD1 conjugation was chosen for the experiments described below. As shown in Figure 8a, SPR measurements

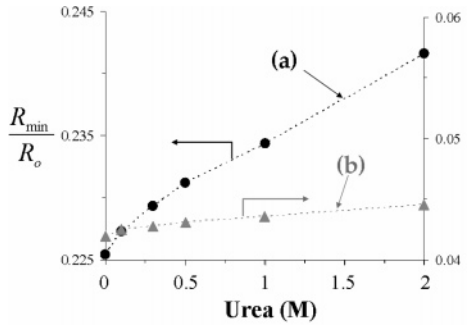

Figure 7. The reflectivity plots of Au thin film with SOD1 in the absence of (a) and presence of (b) adsorbed 20 nm diameter AuNP as a function of urea concentration in the range of 0−2 M.

of AuNP/SOD1/Au indicate an apparent two-state transition with a shift in the pH values of the transition points toward a milder pH than those of the AuNP/SOD1/Au prepared using exposure times of 3 and 12 h. The pH transition of AuNP/SOD1/Au occurs between pH 5 and 7; that is, some degree of control in the operational pH that renders this optical contrast is available by adjusting the exposure time. We also examined the reversibility and stability of the conformational switching process of the AuNP/SOD1 conjugate. Figure 8b shows the reflectivity for the AuNP/SOD1 conjugate as a function of the number of pH cycles. It is clear that the immobilized AuNP/SOD1 conjugate is quite robust and can withstand multiple buffer washings, and that the operation (conformational change) is highly reversible. No reduction in operational amplitude ($\Delta\%R$) is observed after three full cycles, and the magnitude of the reflectivity changes is retained even after 3 weeks. Presumably, the observation that no discernible $\Delta\%R$ reduction was found on the SPR spectrum after the pH cycles suggests that the loss of the attached AuNP caused by the above surface perturbation was negligible.

(33) (a) Chen, W. P.; Chen, J. P. *Surf. Sci.* **1980**, *91*, 601. (b) Pockrand, I. *Surf. Sci.* **1978**, *72*, 577.
(34) Sarkar, D.; Somasundaran, P. *Langmuir* **2004**, *20*, 4657.

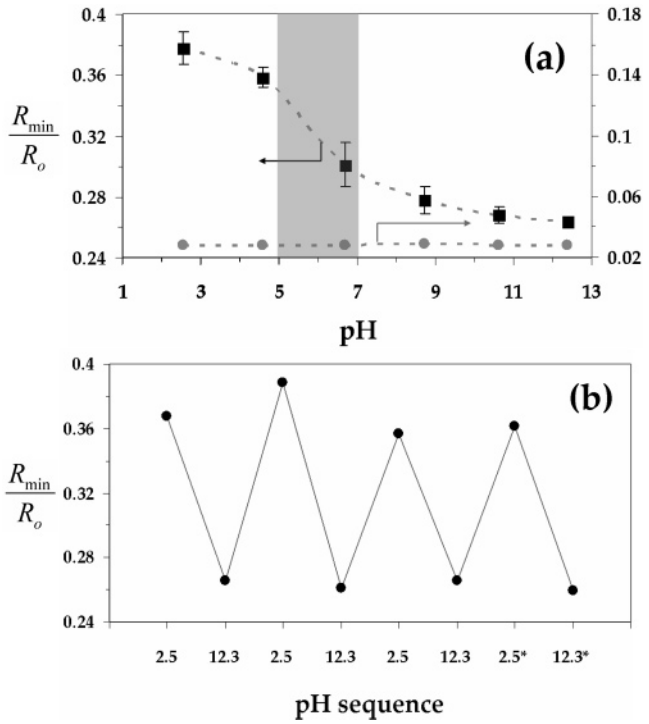

Figure 8. (a) Titration curves of Au thin film with SOD1 in the absence of (gray circle) and presence of (dark square) AuNP for the exposure time and (gray circle) without AuNP. A sigmoidal fit to the titration values is drawn as a dashed line. Error bars show the standard deviation. (b) Switching of the minimum reflectivity (R_{min}/R_o) by the pH change in the AuNP/SOD1/Au. The minimum reflectivity was measured after 3 weeks.

Due to the presence of additional absorbing AuNP, the reflectivity of the system can be expressed in terms of the mean square electric field and the dielectric constants of two absorbing media (Au film and AuNP) by[35]

$$R(\theta) = 1 - \left(\frac{2\pi}{\lambda}\right)\frac{1}{k_{zP}}\{\int_0^{dAu} \mathrm{Im}[\epsilon_{Au}]\langle E_z^{\,2}(\theta)\rangle dz + \int_{d_{Au}+d_{MUA}+d_{SOD1}}^{d_{Au}+d_{MUA}+d_{SOD1}+d_{AuNP}} \mathrm{Im}[\epsilon_{AuNPlayer}]\langle E_z^{\,2}(\theta)\rangle dz\} \quad (1)$$

where $E_z^2(\theta)$ is the mean square electric field in the z-direction (surface normal), λ is the wavelength impinging on the prism/multilayer interface with an angle of incidence θ, ϵ_i is a complex dielectric constant of i layer, and k_{zP} is the z-component of the wave vector in prism and is given by $k_{zP} = (2\pi/\lambda)\cos\theta(\epsilon_p)^{1/2}$. Since the electric field near the resonance angle is very sensitive to changes at the metal/dielectric interface, a minor change in thickness, dielectric constant, or both of the absorbing AuNP layer can significantly alter the electric field amplitude at the interface and its decay pattern, resulting in a change in the reflectivity.

We believe that our observations are a manifestation of stimulus-induced conformational changes of the tethered SOD1 leading to the mechanical movement of the attached AuNP. These conformational changes in the tethered proteins can be accompanied by the movement of the AuNP in either vertical or lateral directions to the surface because it is reasonable to assume that the protein attempts to "stretch" its polypeptide chain on the surface upon unfolding.[36] Figure 9a illustrates the schematic diagram of SPR for the first case, whereas Figure 9b corresponds to the latter case. If, upon a pH-triggered conformational change in the tethered SOD1, the attached AuNP moves horizontally from the Au surface, the reflectivity in the SPR signal would be expected to be unchanged because the horizontal movement of AuNP does not alter the $E_z^2(\theta)$ and $\epsilon_{AuNPlayer}$ but simply induces the rearrangement of AuNP on the SOD1 surface. In contrast, in the latter case, the vertical movement of AuNP results in a variation in both the local dielectric function to the surface normal and $E_z^2(\theta)$ due to the elongation and shortening of the dynamic distance between the Au film and the AuNP, thus affecting the measured reflectivity. Therefore, the changes in the reflectivity in SPR spectra observed here indicate that the AuNP on SOD1 must have moved vertically, but not horizontally, although minor contribution due to horizontal movement cannot be ruled out. If this is the case, the vertical movement of the tethered AuNP should be reflected in the thickness of the AuNP/SOD1 conjugate and be detectable by liquid-AFM. Here we used this technique to directly measure the thickness of the AuNP/SOD1/Au at the two pHs. The result given in liquid-AFM images (Figure S5) shows that, in agreement with the theoretical prediction, although

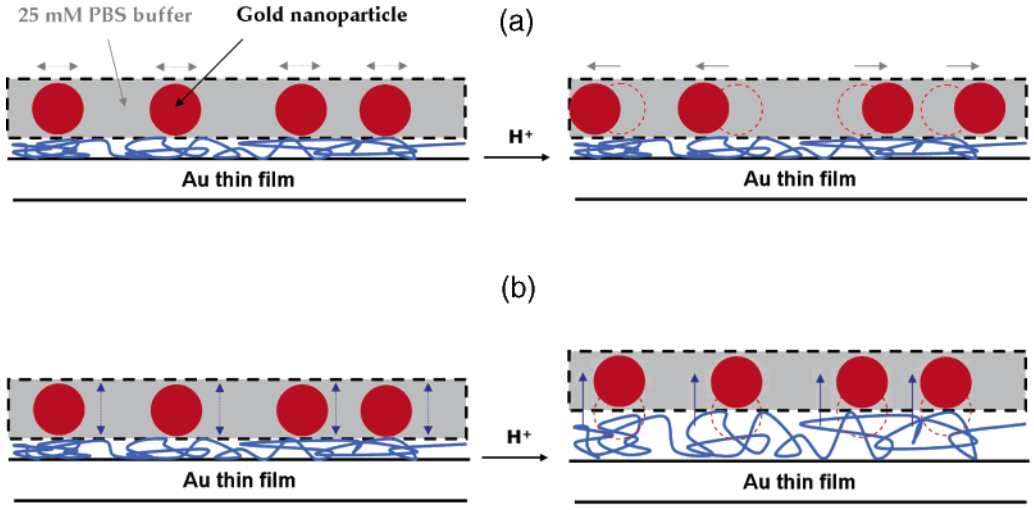

Figure 9. Schematic representation of the switching behavior of the AuNP/SOD1/Au upon exposure to a solution at a low pH. (a) The tethered AuNP attempts to (a) "spread (rearrange) horizontally" and/or (b) "move vertically" on the surface upon the proton-induced conformational changes of SOD1 (not to scale).

there is barely any change in morphology, the height of the AuNP/SOD1/Au at the same location increases by ca. 3 nm when the pH is changed from 7 [due to possible dissolution of the silicon tip at a high pH (>7)] to 2.5. An analogous increase (~4 nm) in the nominal height was also observed for the SOD1/Au upon the urea-driven conformational change.[37] The increase in the thickness is less than expected for SOD1 in the bulk because it has been reported that, upon heat-driven denaturation, the radius of gyration (R_g) of SOD1 in the bulk is increased over its value in the native state by 3-fold.[38] Taking into account the restricted conformational plasticity of the surface-confined SOD1 as the result of the possibility of a tilted orientation, multiple binding (amide bond formation) to the Au surface, and AFM tip compression, this 1.8-fold increase is not unreasonable.

Interestingly, it is noteworthy that, in contrast to findings reported by other groups, the distance dependence of the colloidal AuNP-amplified SPR phenomenon obtained from the experimental geometry (AuNP/SOD1/Au) used here was accompanied by a change in reflectivity without an SPR angle shift under the modulation of the dynamic distance between the AuNP and the Au film. To demonstrate this, we examine the variation in the resonance conditions of AuNP on the Au substrate for various ratios of the distance between them. The extinction efficiency (Q_{ext}) of the AuNP above the Au substrate is given by the sum of these two efficiencies. The formulas for Q_{ext} ($Q_{ext} = Q_{abs} + Q_{scat}$) are[39]

$$Q_{scat} = \frac{k^4[||1 + r_p|\sin\theta\alpha_\perp|^2 + ||1 - r_p|\cos\theta\alpha_{||}|^2]}{6\pi^2 a^2} \quad (2)$$

$$Q_{sbc} = \frac{k}{\pi a^2}\sqrt{\mathrm{Im}^2[|1 + r_p|\sin\theta\alpha_\perp] + \mathrm{Im}^2[|1 - r_p|\cos\theta\alpha_{||}]} \quad (3)$$

respectively, where r_p is the Fresnel reflection coefficient for *p*-polarized beams, k is the wave vector in the ambient, a is the radius of AuNP, and α is the polarizability of AuNP considering the image dipole induced in the substrate and a function of the gap distance between AuNP and the Au substrate (subscripts represent the normal and parallel electric fields). From the above equations, the resonance wavelength of the AuNP above the Au substrate is altered substantially as the gap distance between the AuNP and the Au substrate varies. However, for the case where the ratios of the gap distance to the AuNP radius are in range of 0.4 (pH 12.3) to 0.7 (pH 2.5), the calculated resonance wavelength shift is almost negligible, and instead, Q_{ext} does change appreciably (not shown). This may cause the observed reflectivity change in the SPR spectra because each the resonant wavelength shift and the extinction efficiency can be reflected in the SPR angle shift and the reflectivity, respectively. If this is not the case, other factors, such as (i) surface-roughness-caused light scattering and (ii) the modulated field intensity by the dielectric spacer, must be considered, and the analysis becomes much more complicated. While further quantification of the contribution from each factor was not possible in the current work, our results highlight the importance of the dynamic distance between AuNP and the Au film in dictating the conformational changes of SOD1 at the interface.

Conclusions

In summary, we have designed a new class of surface-immobilized stimulus-responsive hybrid material based on tethered SOD1 on a Au film and with AuNP placed atop SOD1 and clearly demonstrated that a pH-sensitive SOD1/AuNP conjugate can produce an optical contrast through a conformational change when the pH is cycled between 2.5 and 12.3. This vertically lifts and lowers the end-attached AuNP from the Au surface and modulates the dynamic distance between them and, hence, transduces these mechanical motions into changes in the SPR reflectivity driven by the pH.

SPR spectra of AuNP/SOD1 conjugate on Au thin film show a characteristic response to the pH of the surrounding solution. On the other hand, the SOD1/Au without AuNP shows virtually no response toward pH variation. No variation in the SPR curve was observed for the case where alkanedithiol (HDT) replaced the SOD1 as the intervening layer since the latter does not undergo a conformational change upon pH alteration. By virtue of this fact, we attribute the observed changes in the SPR reflectivity to the distance-dependent behavior of the surface-immobilized AuNP, which mirrors the conformational changes of the surface-tethered SOD1 caused by pH variations. This is also evident from the case where the urea replaces the pH. The attachment of AuNP atop SOD1 at even the highest densities led to nonlinear effects in the operational amplitude. Thus, as the results shown here indicate, the attachment of a moderately abundant amount of AuNP created the largest response to repeated pH cycles without any noticeable impairment. The AuNP/SOD1 conjugate could reversibly switch its conformation for multiple runs without any detectable degradation, and its function is preserved after 3 weeks. It can be inferred that the $\Delta\%R$ of 12% as a pH alteration can be easily utilized as an optical "on and off" pH sensor using conventional SPR imaging. Consistent with the theoretical analysis of the SPR response, liquid-AFM images reveal that the switching process is related mainly to the vertical movement of the AuNP/SOD1 upon pH alteration. The reflectivity change can be understood in terms of the distance dependence of the resonance conditions of AuNP on the Au substrate.

This is one of the first examples to show the operation of a substrate-bound protein/AuNP nanodevice based on stimulus-induced conformational changes of protein at an interface and opens up new opportunities for exploiting the intrinsic conformational change of protein that occurs at an interface, for example, to produce nanoscaled mechanical movements, as sensors, and as switches in junctions in response to a stimulus.

Acknowledgment. This work was supported by Grant No. R01-2006-000-10239-0 from the Basic Research Program of the Korea Science & Engineering Foundation. We are also grateful to the Eco-Technopia-21 project of the Korean Ministry of Environment for the financial support.

(35) (a) Harrick, N. J. *Internal Reflection Spectroscopy*; Harrick Scientific Corp.: New York, 1987. (b) Ekgasit, S.; Thammacharoen, C.; Knoll, W. *Anal. Chem.* **2004**, *76*, 561. (c) Ekgasit, S. *Appl. Spectrosc.* **1998**, *52*, 773.
(36) Based on the fact that a $d \sim 20$ nm AuNP is larger than the 4 nm of SOD1, it is unlikely that the length of SOD1 used here would have the ability to wrap around the AuNP.
(37) Kang, T.; Hong, S.; Choi, I.; Yi, J. Unpublished result.
(38) Khare, S. D.; Ding, F.; Dokholyan, N. V. *J. Mol. Biol.* **2003**, *334*, 515.
(39) Okamoto, T.; Yamaguchi, I. *J. Phys. Chem. B* **2003**, *107*, 10321.

Supporting Information Available: Schematic SPR configuration, schematic illustration of the binding reactions, the incident angle-dependent SPR plots obtained from the MUA−Au surface after immobilization of SOD1, TEM image of as-synthesized AuNP and corresponding UV−vis spectrum, and topographical AFM images of the surface of AuNP/SOD1/Au before (pH 7) and after the exposure to pH 2.5 and corresponding typical linear scans along the scan direction. This material is available free of charge via the Internet at http://pubs.acs.org.

JA0632198